Molecular Orientations in Flat-Elongated and Helical Lamellar Crystals of a Main-Chain Nonracemic Chiral Polyester

Christopher Y. Li,[†] Stephen Z. D. Cheng,*[,†] Jason J. Ge,[†] Feng Bai,[†] John Z. Zhang,[†] Ian K. Mann,[†] Lang-Chy Chien,[‡] Frank W. Harris,[†] and Bernard Lotz[§]

Contribution from The Maurice Morton Institute and Department of Polymer Science, The University of Akron, Akron, Ohio 44325-3909, Liquid Crystal Institute, Kent State University, Kent, Ohio 44010-0001, and Institute Charles Sadron, 6 Rue Boussingault, Strasbourg 67083, France

Received September 7, 1999

Abstract: Single flat-elongated and helical lamellar crystals have been grown thermotropically in a main-chain nonracemic chiral liquid crystalline polymer that was synthesized from (*R*)-(−)-4′-{ω-[2-(*p*-hydroxy-*o*-nitrophenyloxy)-1-propyloxy]-1-nonyloxy}-4-biphenyl carboxylic acid, PET(R*)-9. The crystals possess the identical orthorhombic lattice dimensions of $a = 1.07$ nm, $b = 0.48$ nm, and $c = 5.96$ nm.[1,2] Dark field (DF) image, bright field image, and selective area electron diffraction (SAED) experiments using transmission electron microscopy (TEM) provide chain orientation information in both of these crystals. In the flat-elongated lamellar crystals, the chain direction is perpendicular to the substrate surface in a center zone along the long (*b*) axis of the crystals. Moving away from this zone along the short (*a*) axis of the crystal, the chain direction continuously tilts in the *ac*-plane. A small tilt of approximately 0.002° per molecular layer is estimated using the SAED results. In the helical lamellar crystals, the main twist direction is parallel to the helical axis, and the rotation angle for each molecular layer is approximately 0.05°. However, specifically designed DF experiments using the entire and partial (205) and (206) diffraction arcs show that the chain orientation direction is also twisted along the short helical axis of the lamellar crystal. The rotation angle is approximately 0.01° per molecular layer. Therefore a second twist direction with a changing molecular orientation exists in addition to the long helical axis of the crystal. Based on these experimental observations, the concept of a *double-twisted* molecular orientation in the helical lamellar crystal can be established, although in principle, the macroscopic translational symmetry is broken along both of the long and short axes of the helical lamellar crystals in Euclidean space.

Introduction

Chirality in molecules has generated profound new phase structures, transition behaviors, and specific optical and electric properties in low molecular mass liquid crystals. These involve structural hierarchies of chirality with different length scales ranging from molecules to a final supermolecular assembly (Figure 1) and transferring of chiralities from one structural level to another. Asymmetrical chiral centers introduced into a polymer backbone, which is a *primary* chiral structure (configurational chirality), usually result in helical macromolecular conformations (a *secondary* chiral structure, conformational chirality). When the polymer chains with helical conformations pack together following symmetric schemes to form ordered structures, the chirality breaks the local mirror symmetry and may lead to a helical morphology (a *tertiary* chiral structure, phase chirality) depending on the type of structural ordering formed. This has been observed in low ordered liquid crystalline (LC) phases, such as in the cases of cholesteric (Ch),[3,4] twist grain boundary smectic A (TGBA),[5−8] chiral smectic C (S_C*),[9] and blue phases (BP).[10] In the helical morphologies of Ch[3,4] and TGBA phases,[5−8] the molecular chain direction is perpendicular to the helical axis, while in S_C* phases, there is an acute angle between the molecular axis and the helical axis.[9] A helix has also been identified in BPs in which the direction of a helical axis changes with respect to the molecular chain direction.[10]

It is generally understood in synthetic condensed matter that tertiary helical structures have only been found in low-ordered phases of small molecular liquid crystals. As the structural order increases to form highly ordered LC phases (such as smectic crystal G*, H*, J*, and K* phases), the helical morphology is expected to be suppressed.[11] This is due to the fact that interaction upon helical packing is typically lower compared to the interaction of forming high-ordered phases which require a parallel close packing scheme (such as during crystallization).[11] Hence, the helical morphology cannot be observed in these highly ordered smectic crystal phases in chiral liquid crystals, and their phase morphology shows no difference compared with their nonchiral counterparts. Recently, however, a helical single

* To whom correspondence should be addressed. E-mail: cheng@polymer.uakron.edu.
† The University of Akron.
‡ Kent State University.
§ Institute Charles Sadron.

(1) Li, C. Y.; Yan, D.; Cheng, S. Z. D.; Bai, F.; He, T.; Chien, L. C.; Harris, F. W.; Lotz, B. *Macromolecules* **1999**, *32*, 524−527.
(2) Li, C. Y.; Yan, D.; Cheng, S. Z. D.; Bai, F.; Ge, J. J.; He, T.; Chien, L. C.; Harris, F. W.; Lotz, B. *Phys. Rev. B* **1999**, *60*, 12675−12680.
(3) Friedel, G. *Ann. Phys.* **1922**, *18*, 273−474. Saupe, A. *Angew. Chem., Int. Ed.* **1968**, *7*, 97−112.
(4) Buckingham, A. D.; Ceasar, G. P.; Dunn, M. B. *Chem. Phys. Lett.* **1969**, *3*, 540−541.
(5) de Gennes, P. G. *Sloid State Commun.* **1972**, *10*, 753−756.
(6) Renn, S. R.; Lubensky, T. C. *Phys. Rev. A* **1988**, *38*, 2132−2147.
(7) Goodby, J. W.; Waugh, M. A.; Stein, S. M.; Chin, E.; Pindak, R.; Patel, J. S. *J. Am. Chem. Soc.* **1989**, *111*, 8119−8125.
(8) Goodby, J. W.; Waugh, M. A.; Stein, S. M.; Chin, E.; Pindak, R.; Patel, J. S. *Nature* **1989**, *337*, 449−452.
(9) Helfrich, W.; Oh, C. S. *Mol. Cryst. Liq. Cryst.* **1971**, *14*, 289−292.
(10) Saupe, A. *Mol. Cryst. Liq. Cryst.* **1969**, *7*, 59−74.
(11) Goodby, J. W.; Slaney, A. J.; Booth, C. J.; Nishiyama, I.; Vuijk, J. D.; Styring, P.; Toyne, K. J. *Mol. Cryst. Liq. Cryst.* **1994**, *243*, 231−298.

10.1021/ja993249t CCC: $19.00
Published on Web 12/18/1999

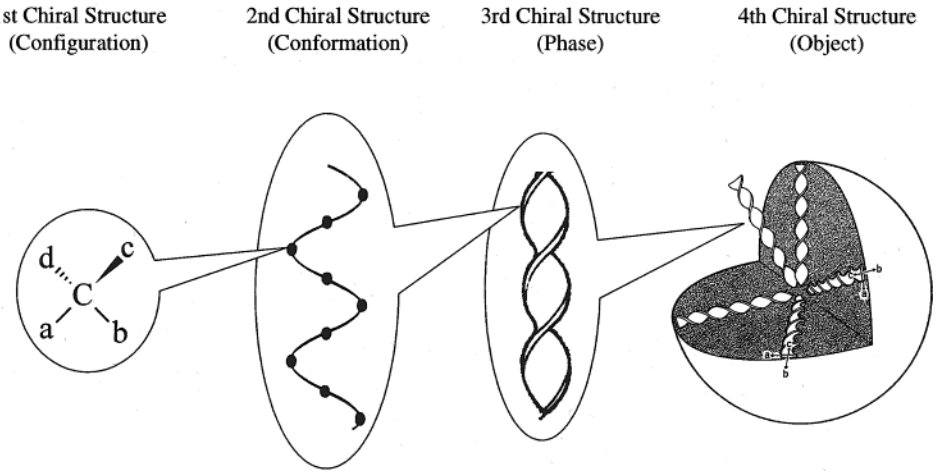

Figure 1. Schematic drawing of four different levels of chirality in polymers.

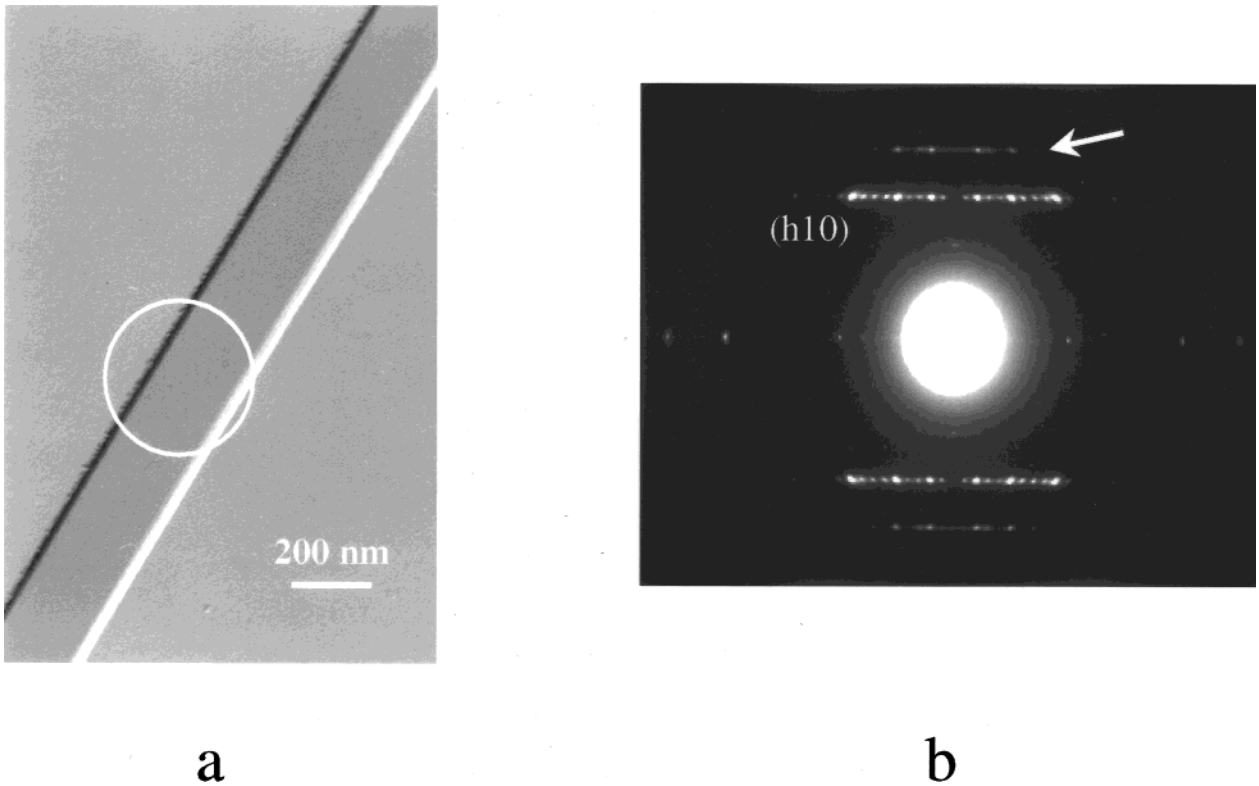

Figure 2. A BF image of a flat-elongated lamellar crystal (a); a SAED pattern having the [00*l*] zone (b). The ED pattern originates from the circled area in (a).

lamellar crystal has been thermotropically grown in one main-chain chiral LC polyester. To our knowledge, this is the first time that the phase chirality with a helical morphology can be preserved in the crystalline state of synthetic polymers.[1,2]

Crystalline chiral polymers usually form banded spherulites due to cooperative lamellar twisting, which is one example of the highest level of chiral structure.[12,13] If the twisted lamellar crystals in spherulites are considered as a tertiary chiral structure, their spherulitic "aggregates" can be identified as *quaternary* chiral structure, which is related to the object chirality. It has been frequently speculated that this banded texture must be associated with the chiral configurations in the polymer chains. For example, in poly(hydroxybutyrate) (PHB), which is obtained from its natural bacterial source and known to be the *R*(−) enantiomer, the twist in the PHB banded spherulites is left-handed.[12] In poly(propylene oxide), the *R*(−) enantiomers generate right-hand twist, while the *S*(+) enantiomers give left-hand twist in the banded texture. In a 50:50 mixture of *R*(−) and *S*(+) enantiomers, the banded texture disappears in the spherulites.[14] Therefore, the chiral configurations in the polymer backbones should play an important role in the formation of the banded texture in spherulites.

However, as shown in Figure 1, attempts to relate the primary chiral structure with the quaternary chiral structure without knowing the secondary and tertiary chiral structures is an incomplete practice. In other words, *transferring from one chirality hierarchy to another need be neither automatic nor*

(12) For a recent summary, see: Keith, H. D.; Padden, F., Jr. *Macromolecules* **1996**, *29*, 7776−7786.

(13) Briber, R. M.; Khoury, F. A. *J. Polym. Sci. Polym. Phys. Ed.* **1993**, *31*, 1253−1272.

(14) Singfield, K. L.; Hobbs, J. K.; Keller, A. *J. Cryst. Growth* **1998**, *183*, 683−689.

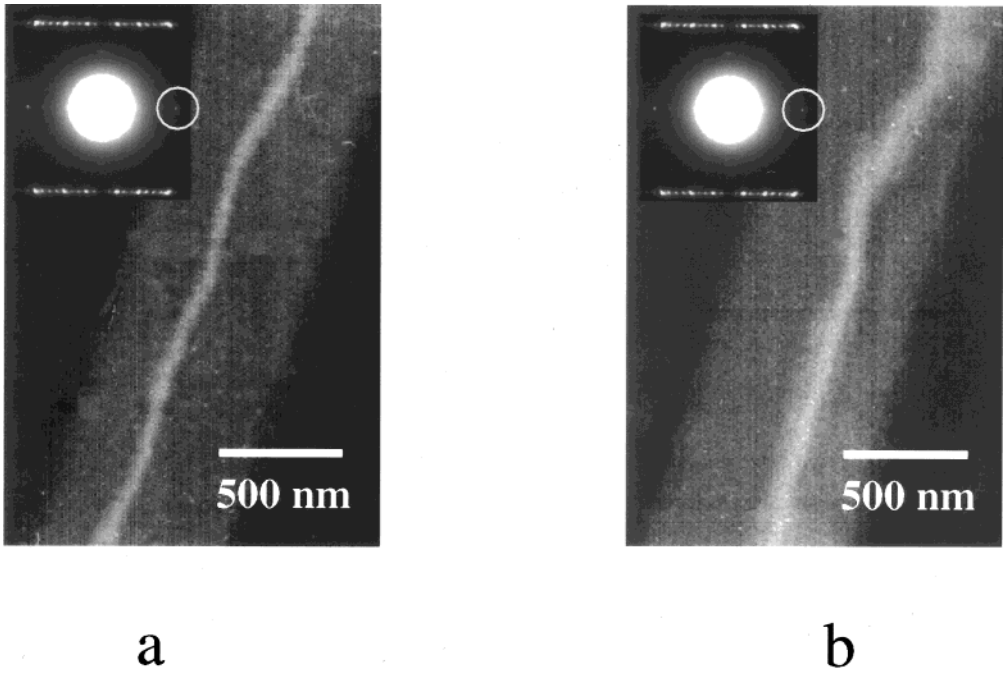

Figure 3. A (200) DF image of a flat lamellar crystal (a) with an insert of the ED pattern; a (200) DF image of the same crystal after a 1°-rotation around the *b*-axis of the crystal.

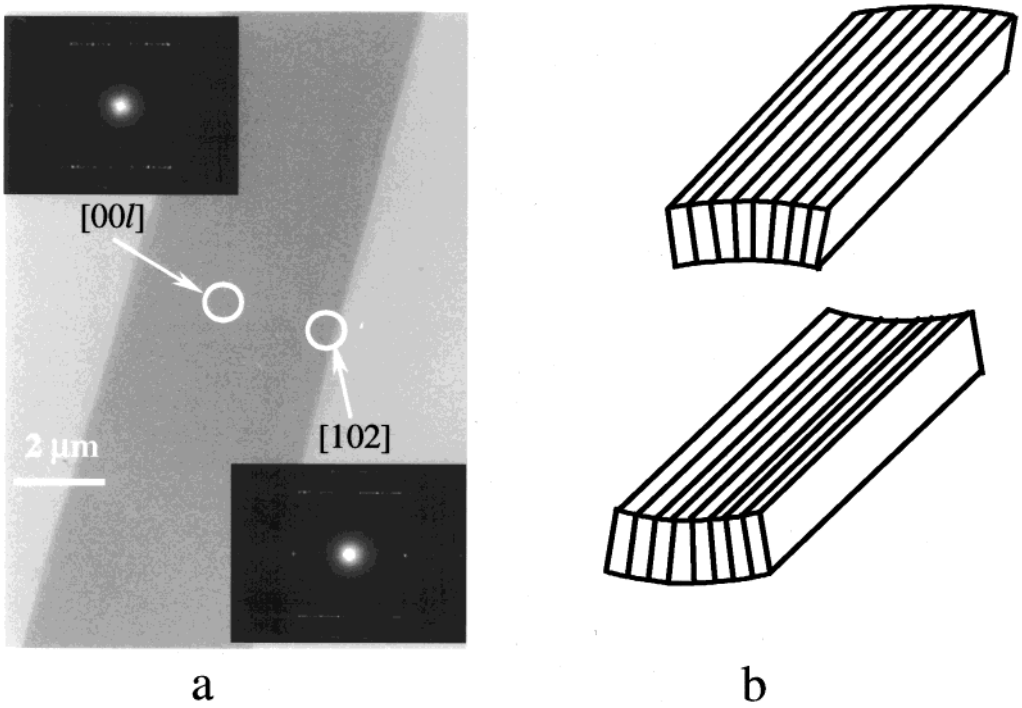

Figure 4. Two SAED patterns from different sites of a fully developed flat lamellar crystal (a); schematic drawing of the chain orientation directions in the flat-oriented crystal (b).

necessary. Establishing quantitative links between the configurational chirality and objective chirality requires information on the conformational and phase chiralities. Furthermore, configurational chirality is not necessarily the only cause of lamellar twisting. An example is nonchiral polyethylene (PE). The corresponding structural asymmetry in these lamellar crystals causes a significant longitudinal bending moment in the crystals and introduces the lamellar twisting.[15]

It is important to note that for almost all of the reported polymers showing banded spherulites, namely, quaternary chiral structures, the tertiary chiral structures in these materials have not been isolated. In fact, a recent study shows that unlike their banded spherulite, lamellar single crystals of optically active *R*(−) or *S*(+) poly(epichlorohydrin) grown from dilute solution are flat in shape and possess no helical morphology.[16,17] In other words, the conformational chirality has not been transferred to the phase chirality, and thus the chiral memory is somehow lost between these two structural hierarchies.

(15) Keith, H. D.; Padden, F. Jr.; Lotz, B.; Wittmann, J. C. *Macromolecules* **1989**, *22*, 2230−2238.

(16) Singfield, K. L.; Brown, G. R. *Macromolecules* **1995**, *28*, 8006−8015.

(17) Saracovan, I.; Cox, J. K.; Revol J.-F.; Manley R. St. J.; Brown, G. R. *Macromolecules* **1999**, *32*, 717−725.

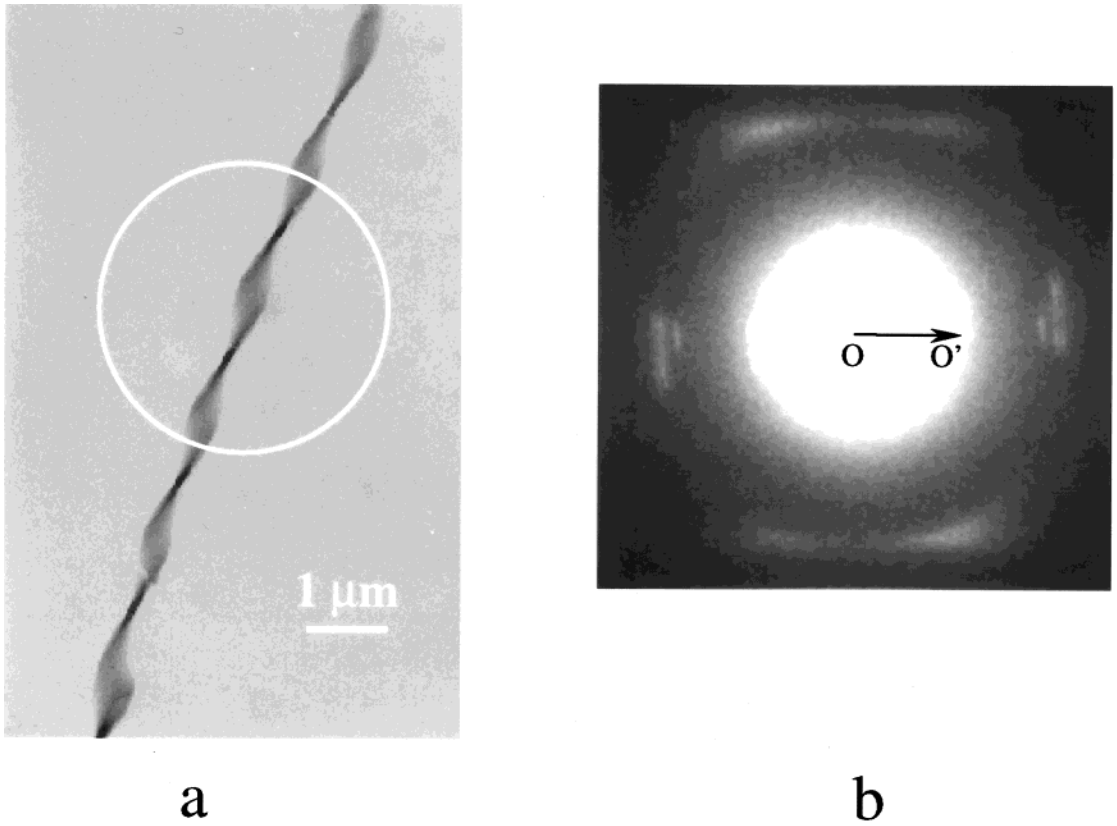

Figure 5. A BF image of a helical lamellar crystal (a) and its corresponding SAED pattern obtained in the circled area (b).

We have often speculated that it is possible to synthesize main-chain nonracemic chiral LC polymers with relatively rigid backbones to maintain the chiral memory when the structure transfers from the secondary to tertiary structure in a highly ordered crystalline phase. If the free energy of the helical chiral packing is comparable to that of the chain parallel ordering, the helical morphology may be preserved. In our recent observations in a nonracemic chiral LC polyester, the intriguing phenomenon is that not only can both the flat-elongated and the helical lamellar crystals coexist during crystallization, but they also possess the same crystal lattice and unit cell dimensions, although the macroscopic translational symmetry is broken in the helical lamellar crystal.[1,2] The crystal structure in both of the lamellar crystals has been determined to be identical. It is orthorhombic, having dimensions of $a = 1.07$ nm, $b = 0.48$ nm, and $c = 5.96$ nm.[1,2] The short and long axes of the flat-elongated lamellar crystal have been identified to be parallel to the *a*- and *b*-axes of the crystal unit cell. The experiments using low molecular mass PE decoration[18,19] have demonstrated that the chain folding direction in the flat-elongated lamellar crystals is along the long (*b*) axis while the folding direction of the helical lamellar crystal is along the long helical axis.[1,2] In this publication, dark field (DF) experiments for both types of crystals in transmission electron microscopy (TEM) are reported. A combination of bright field (BF) and select area electron diffraction (SAED) experiments show that chain orientations in the flat-elongated and helical lamellar crystals can be determined. Specifically designed DF experiments provide evidence that the chain orientation in the helical lamellar crystals is *double-twisted*.

Experimental Section

Materials and Sample Preparation. The polymer reported here was synthesized from (*R*)-(−)-4′-{*ω*-[2-(*p*-hydroxy-*o*-nitrophenyloxy)-1-propyloxy]-1-nonyloxy}-4-biphenyl carboxylic acid. The detailed synthesis routes of the monomers and polymers have been published elsewhere.[1,2,20] The number of methylene units in the polymer of this study is nine, and this polymer possesses right-hand chiral centers (R*) along the main-chain backbone and is thus abbreviated as PET(R*)-9. Its chemical structure is given here. The specific rotation of the

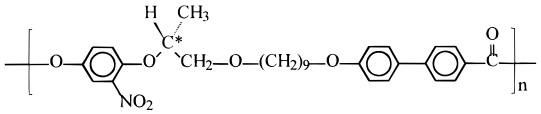

monomers is $[\alpha]_D$ −28.5°. Due to the head-to-tail connection of the monomers in this polymer backbone (an A−B monomer polymerization),[1,2,20] the optical activity of this monomer is retained, and thus, the polymer is nonracemic chiral. The molecular weight of PET(R*)-9 is approximately 16000 g/mol and the polydispersity is approximately 2 after fractionation, as measured by gel permeation chromatography based on polystyrene standards.

Polymer thin films (with a thickness of 50−100 nm) were prepared via solution casting from a 0.05% (w/v) tetrahydrofuran solution. After the solvent was evaporated, the films were heated on a heating stage (Mettler FP-90) above its highest endothermic transition temperature (190 °C) and the reaction was subsequently quenched to preset temperatures and held isothermally for various periods ranging from several minutes to a few days. The samples were then quenched in liquid nitrogen and equilibrated at room temperature, which is below the glass transition temperature of this polymer ($T_g = 37$ °C). The thin film samples prepared for TEM observations were first examined with polarized light microscopy and phase contrast microscopy before they were shadowed by Pt and coated with carbon for TEM observations.

(18) Wittmann, J. C.; Lotz, B. *Makromol. Rapid Commun.* **1982**, *3*, 733−738.

(19) Wittmann, J. C.; Lotz, B. *J. Polym. Sci. Polym. Phys. Ed.* **1985**, *23*, 205−226.

(20) Bai, F.; Chien, L. C.; Li, C. Y.; Cheng, S. Z. D.; Percheck, R. *Chem. Mater.* **1999**, *11*, 1666−1671.

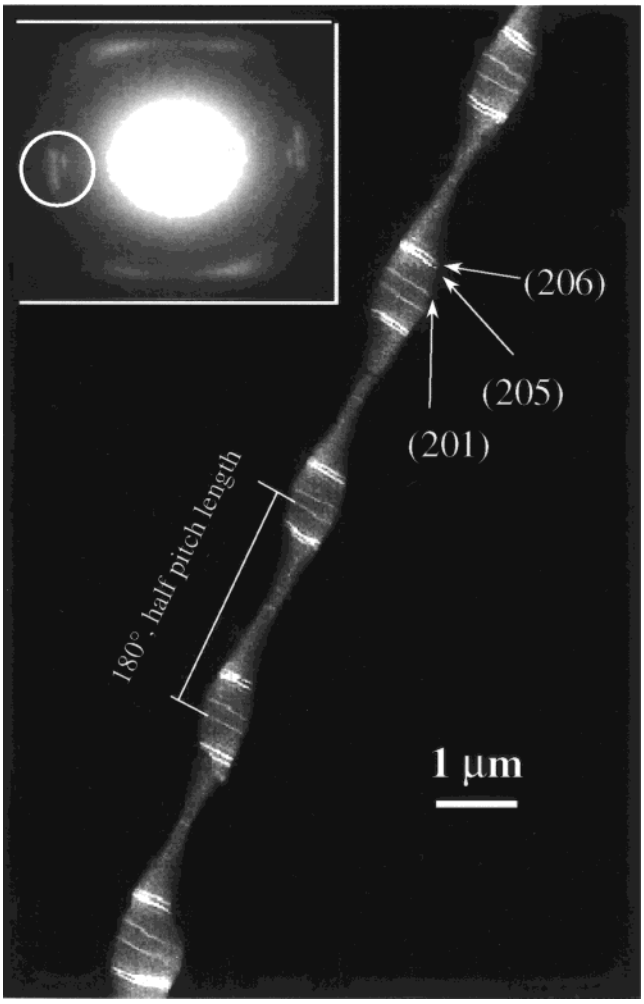

Figure 6. A DF image of a helical lamellar crystal using the entire (201), (205), and (206) diffraction arcs. The diffraction arcs are circled in the SAED patterns and inserted in this figure.

The shadowing process was not performed on the samples used for the DF experiments.

Equipment and Experiments. TEM experiments were carried out in a JEOL (1200 EX II) TEM using an accelerating voltage of 120 kV. SAED patterns of the samples having different zones were also obtained using a TEM tilting stage to determine the three-dimensional sizes of the crystal unit cell. Calibration of the ED spacing was done using TlCl in a *d* spacing range smaller than 0.384 nm, which is the largest spacing for TlCl. Spacing values larger than 0.384 nm were calibrated by doubling the *d* spacing of those diffractions based on their first-order diffractions. DF experiments were performed using a diffraction mode of TEM. Selective DF images were obtained using specific (*hkl*) electron diffractions to observe the chain orientations in both the flat-oriented and helical lamellar crystals. The tilting stage was also used in the DF experiments.

Results and Discussion

Chain Orientations in the Flat-Elongated Lamellar Crystals. PET(R*)-9 can be crystallized to form both the flat-elongated and helical lamellar crystals within a certain crystallization temperature region as reported previously.[1,2] Figure 2a is a BF image illustrating the PET(R*)-9 flat-elongated lamellar crystal morphology and Figure 2b shows a SAED pattern having a [00*l*] zone from the circular area of Figure 2a as also reported previously. In particular, the (*h*10) layer intensities are strong. Comparing the (*h*10) layer with the (*h*00) layer in the ED pattern having the [00*l*] zone in Figure 2b, the diffractions of the (*h*10) layer are five times denser than that of the *a**-aixs of the basic unit given by the (*h*00) layer diffractions. This may indicate that commensurate structures exist and they are superimposed on the basic unit cell along the *a*-axis with a periodicity five times larger than the *a*-dimension of the unit cell.[1,2] There is another parallel diffraction layer (the arrow in Figure 2b) above the (*h*10) layer. The distance between this layer and the (*h*10) layer is one-third of that between the (*h*00) and the (*h*10) layers. The simplest explanation of this observation is that there is a commensurate structure along the *b*-axis that has a spacing three times larger than the *b*-dimension of the basic unit cell.[1,2]

Figure 3a shows a DF image of this lamellar crystal using the (200) diffraction [taken from the (200) diffraction spot circled in the ED pattern inserted]. The most surprising feature in Figure 3a is the observation of a bright zone along the long (*b*) axis of the lamellar crystal. Molecular chains in this bright zone of the crystal satisfy Bragg's law and possess the same orientation direction parallel to the electron beam (the substrate surface normal). The bright zone shifts along the short axis of the crystal if the sample is rotated along the crystal *b*-axis during DF observation. Figure 3b is, for example, obtained after a 1°-rotation along the long (*b*) axis of the lamellar crystal shown in Figure 3a. This 1°-rotation causes a shift of the bright band in the DF image toward the right edge of this lamella. Our previous tilting experiments have shown that the angle between the (200) and (201) planes is 5° with respect to the rotation of the *b*-axis,[2] therefore, a 1°-rotation should not bring a new zone into the ED pattern.[2] This suggests that the chain direction in the new bright zone observed in Figure 3b is tilted approximately 1° toward the short (*a*) axis with respect to that in the original bright zone seen in Figure 3a.

The above analysis can be supported by the SAED observations. For a fully developed lamella, the size along the short (*a*) axis can reach 5 μm (Figure 4a). The SAED pattern with the [00*l*] zone can be observed as shown in Figure 2b when this pattern is taken from the circle on the near center of the crystal. This reveals that within the circular area, the chains have their direction parallel to the electron beam.[1,2] When the aperture is moved along the long (*b*) axis, the ED pattern maintains the [00*l*] zone. However, when the aperture is moved along the short (*a*) axis (toward the right side of the crystal in Figure 4a), a [102] zone ED pattern is observed (attached in Figure 4a). This indicates that molecular chains tilt 5° along the short (*a*) axis from the near center to the right side area of the crystal. Therefore, it can be deduced that along the short (*a*) axis of the lamellar crystals, the chains are not exactly parallel to each other. Instead, moving from the near center zone of the crystal to the elongated edges along the *a*-axis, the molecular chains continuously and slightly tilt away from the basal substrate normal. The overall tilt across half of the length along the short axis (2.5 μm) is approximately 5°. The tilt angle of each molecular layer can thus be roughly calculated using information about the overall tilt angle and the shifted distance along the short axis between two bright zones before and after tilting. Since the *a*-dimension of the unit cell is 1.07 nm, one can deduce that there is approximately 0.002° tilt per molecular layer along the *a*-axis (toward both of the edges) in the *ac*-plane. A schematic model drawn to describe the chain direction in the flat-elongated lamellar crystal is shown in Figure 4b, in which the chain orientations are schematically illustrated.

Chain Orientations in the Helical Lamellar Crystals. It is certainly most interesting and necessary to examine the chain orientations in the helical lamellar crystals. Figure 5a is the BF image of a helical lamellar crystal. A typical SAED pattern (from the circle in Figure 5a) is shown in Figure 5b. Sharper

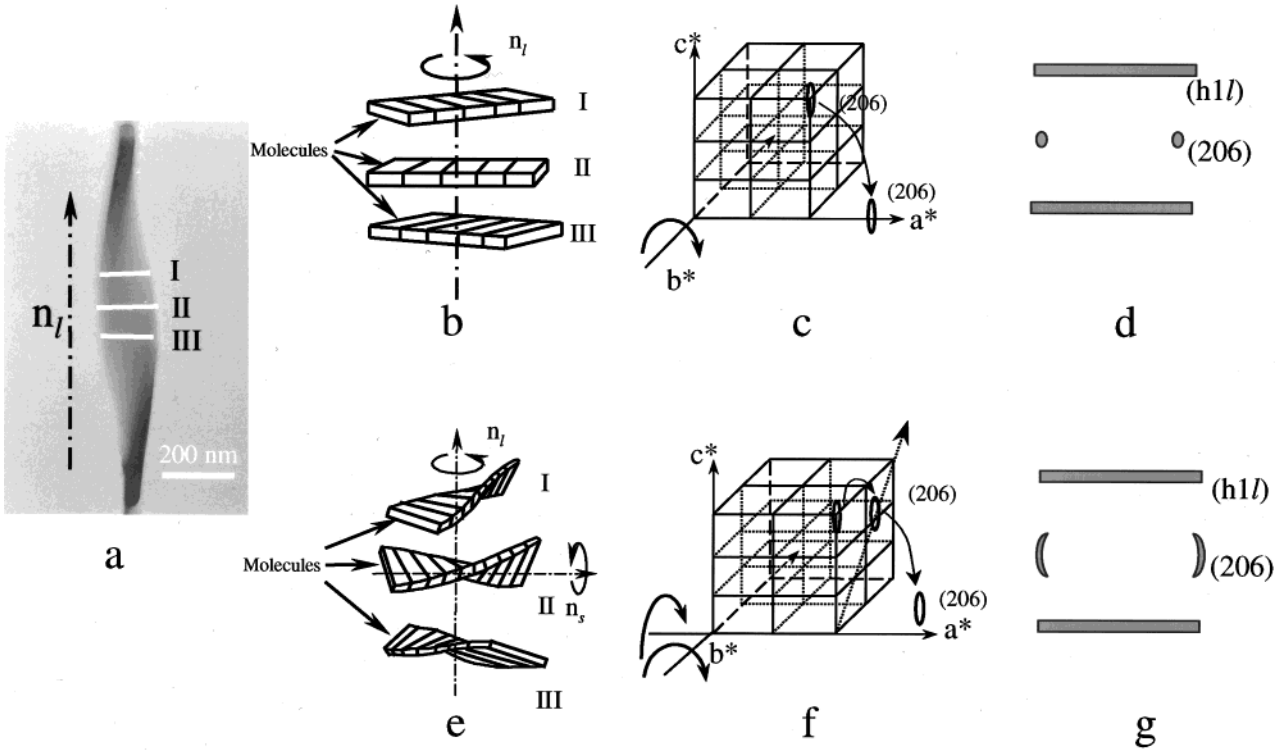

Figure 7. Schematic drawings of two (single- and double-) twist models of the helical lamellar crystal. The (206) diffraction is used to illustrate the formation of the SAED pattern experimentally observed by rotating the *b**-axis (for the single-twisted model) or both the *a**- and *b**-axes (for the double-twisted moel) in the unit cell reciprocal lattice. In this figure, part a shows the helical lamellar crystal with three cross-sections, I, II, and III, which generate the (200) and (206) diffractions. Parts b−d correspond to the single-twist model. Part b is the individual cross-sections (I, II, and III) in which I and III are rotated ±30° with respect to II; part c corresponds to a single rotation of the reciprocal lattice along the *b**-axis to generate the (206) diffraction; and part d is the resulting ED pattern. Parts e−g illustrate the double-twist model. Part e is the individual twisted cross-sections (I, II, and III) in which I and III are rotated ±30° with respect to II; part f corresponds to double rotation of the reciprocal lattice along both the *a**- and *b**-axes to generate the (206) diffraction, and part g is the resulting ED pattern.

SAED patterns can also be obtained to determine the unit cell structure as described in refs 1 and 2. The special feature of this SAED pattern is the three diffraction arcs located on the equatorial (the horizontal line) of the ED pattern (parallel to the short axis of the helical lamellar crystal). These arcs are asymmetric with respect to the equatorial in this ED pattern, implying that the helical crystal deviates from a perfect rotational symmetry with respect to the long helical axis. This may be due to the restriction of the substrate during the helical crystal growth, since the upper crystal regions can grow more readily in the lateral direction compared with the lower region. Based on the unit cell dimensions determined,[1,2] these three arcs correspond to the (201), (205), and (206) diffraction planes, which are the strongest among all of the (20*l*) diffractions.[2] On the other hand, two sets of very diffuse diffraction streaks are symmetrically located above and below the central horizontal line of the SAED (the OO′ line in Figure 5). These belong to the dense (*h*1*l*) diffractions.

Figure 6 is a DF image obtained from the entire (201), (205), and (206) diffraction arcs of a helical lamellar crystal. The circle on the SAED pattern inserted in this figure illustrates the diffraction arcs used for the DF experiment. It is clearly observed that in a half-pitch length, two sets of narrow, bright bands (three bands in each set) exist along the short axis of the helical lamellar crystal (in flat crystals, the bands are along the crystal long axis), and appear periodically along the long helical axis of the crystal with a periodicity equal to the half-pitch length. The distribution of the bands along the helical crystal implies that they are attributed to the (201), (205), and (206) diffractions. This is because the length of a half-pitch along the long helical axis corresponds to a 180° rotation of the helical lamellar crystal (Figure 6), and the three bright bands tilt approximately 5°, 25°, and 30° with respect to the substrate which will give rise to these three diffractions respectively; based on the crystal unit dimension, there is about 5° between [200] and [201]. The observation shows that the twist is continuous. Furthermore, the rotation angle of the chains between adjacent molecular layers can be calculated to be approximately 0.05° along the long helical axis.

To explain both the arc-shape ED (Figure 5b) and DF (Figure 6) results, we assume first a single-twist model of the chain orientation (Figure 7), which is the simplest approach to generate a helical morphology such as in the case of a Ch phase. In this model, there is only one twist axis representing the long helical (n_l) axis and the chains are parallel to each other in the cross section of the crystal. Three individual cross sections of a helical crystal, denoted as I, II, and III in Figure 7a, are individually separated and shown in Figure 7b. There is ±30° rotation along the n_l axis of cross sections I and III with respect to II. If the II cross section provides the [00*l*] zone in the ED pattern, I and III cross sections should give rise to both the [301] and [30$\bar{1}$] zones. The corresponding reciprocal lattice should rotate ±30° along the *b**-axis as shown in Figure 7c. This thus leads to a pair of (206) diffractions on the central horizontal line (Figure 7d). However, this model does not generate the diffraction arcs as observed in the SAED of Figure 5b, suggesting that the chain orientation in the helical crystals is more complicated than the single-twist geometry.

A double-twist model is thus proposed. The difference between the single-twist and the double-twist is that in the latter model, the cross section of the crystal is also twisted. Hence, the molecular directions possess two twisted axes along both

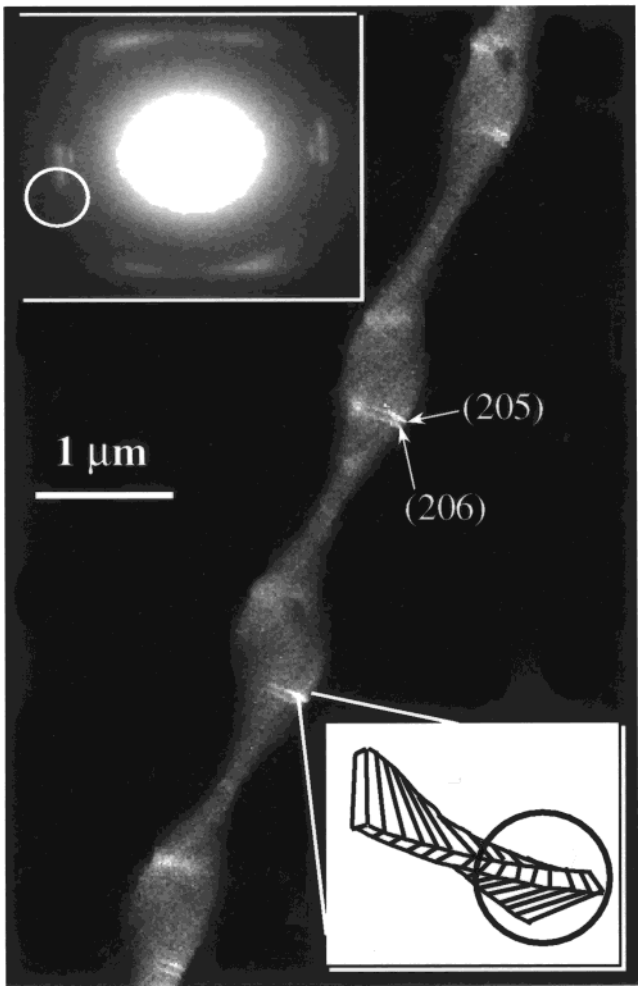

Figure 8. A DF image of a helical lamellar crystal using the partial (205) and (206) diffraction arcs. The circled parts of the diffraction arcs in the ED pattern are inserted in this figure. Note that the (201) diffraction is not included in the ED circle, and therefore, the bright band corresponding to this diffraction is not observed in this DF image.

the long and short helical (n_l and n_s) axes, respectively (Figures 7e and 7f). In this case, the central portions of I and III cross sections provide the [301] and [30$\bar{1}$] zones in the ED pattern as in the single-twist model, which results in the (206) diffraction appearing on the center horizontal line. Moving from the center to both of the edges within the I and III cross sections, the generated (206) diffractions gradually deviate from this line due to the molecular twist along the n_s axis. Figure 7f shows the corresponding rotations along both the *a**- and *b**-axes in the reciprocal lattice to visualize this double-twist. Note that the *a**-axis rotation along the n_s axis is continuous and the rotation angle is determined by the azimuthal angle of the SAED diffraction arc (Figure 5b). For these three diffraction arcs, the rotation angle is close to 20° from the left to right edges across the n_s axis. Therefore, chains in each molecular layer are rotated with respect to the n_s axis direction by an angle of approximately ±0.01°. The resulting schematic ED pattern with a pair of (206) diffraction arcs is presented in Figure 7g. The same principle can be applied to explain the arc shapes of the (201) and (205) diffractions.

Although it seems that the double-twisted model can explain the arc-shape of the (201), (205), and (206) diffractions, Figure 6 alone cannot uniquely determine if the molecular orientation in the helical lamellar crystal is single- or double-twisted. To provide experimental evidence of the double-twist chain orientaiton in the crystals, we have specifically designed an experiment using partial (205) and (206) diffraction arcs to construct the DF image as shown in Figure 8. Note that the circled area selected in the ED pattern (insert in Figure 8) does not include the (201) diffraction arc, and therefore, the bright band corresponding to the (201) diffraction arc in Figure 6 is not observed. More importantly, only portions of the (205) and (206) bright bands appear along the n_s axis of the helical lamellar crystal. This indicates that every diffraction spot along the azimuthal direction of the diffraction arc must quantitatively correspond to the positions along the bright band. For example, the bottom half of the (205) and (206) diffraction arcs circled in Figure 8 correspond to the bright bands appearing in the right sides of the long helical edge. If this helical lamellar crystal is perfectly symmetric, the bright bands of these two half diffraction arcs should alternatively appear at both the right and left sides of the long helical edge. In Figure 8, we only observe diffuse traces of these bands in the left side, which are not as clear as those in the right side of the long helical edge. As discussed previously, this is likely due to the imperfect rotational symmetry of the helical crystals which are restricted by the substrate. However, it does not obscure our main point that the chain orientation in the bright bands of the DF images is continuously twisted with respect to the n_s axis as predicted by the double-twist model.[21,22]

We predict that when a lamellar crystal twists to form a helix, two edges of the lamella have to possess the largest deformation and highest chain rotation angle in the lamella. The consequence of these deformations and chain rotation is to bring instability to the crystal formation and limit the size of the crystal along the short helical axis. The formation of these helical lamellar crystals exhibits a combination of two spontaneous translational symmetry-breaking processes along both the long and short helical axes on a macroscopic scale. These are incompatible with the conventional crystalline structural repetition scheme, which commonly requires parallel chain packing. Therefore, this helical lamellar crystal is symmetrically "soft" rather than a true crystal based on the traditional crystal definition in Euclidean space. Mathematically, it can only be a true crystal in Riemannian space.[23] How these double-twisted lamellar crystals pack with each other to form a quaternary structure in a three-dimensional space is still an open question for further study. In principle, this packing requires introducing periodic defects as proposed in BPs.

Conclusion

In summary, the DF results combined with the BF and SAED experiments in TEM have provided important observations to determine the chain orientations in both the flat-elongated and helical lamellar crystals. It is surprising that in the flat-elongated lamellar crystal, the chain orientation direction is parallel to the

(21) Li, C. Y.; Cheng, S. Z. D.; Ge, J. J.; Bai, F.; Zhang, J. Z.; Mann I. K.; Harris, F. W.; Chien, L.-C.; Yan, D.; He, T.; Lotz, B. *Phys. Rev. Lett.* **1999**, *83*, 4558−4561.

(22) One of the reviewers proposed that "It does not seem necessary to invoke 'double-twisting' to explain the experimental results. In particular, complete twisting of the crystal about the *a*-axis would lead to chains which were no longer nominally normal to the lamellar surface. It seems more likely there would be only limited twisting of this sort, in fact of the bending type seen in the earlier dark field experiments. Such bending could also explain the dark field images give in Figure 8, since they could cause a rotation of the crystal sufficient to put it out of the Bragg condition on one-half of the crystal with respect to the other. It seems that an alternative explanation which would capture most of the experimental results is to have single-twist of a slightly bent lamellar crystal." Based on our ED and DF image results, the readers should make their own judgments.

(23) Kleman, M. *Adv. Phys.* **1989**, *38*, 605−667.

electron beam direction only in the near center zone of the crystal along the long (*b*) axis. A gradual tilt of the chain direction along the short (*a*) axis in the *ac*-plane can be found with a tilting angle of about 0.002° per molecular layer. On the other hand, DF images of the entire (201), (205), and (206) diffraction arcs show sets of bright bands which periodically appear along the long helical axis of the crystal. A specifically designed DF image experiment using partial (205) and (206) diffraction arcs provides the positional correspondence between these ED arcs along the azimuthal direction and the (205) and (206) bright bands. This proves that the chain orientation in the helical lamellar crystal is double-twisted along both the long and short helical axes. The rotation angle along the long helical axis is approximately 0.05° per molecular layer, while the tilting angle along the short axis is about 0.01°. Based on our knowledge, this is the first experimental observation in proving the double-twisted chain orientation and establishing this concept in helical lamellar crystals.

Acknowledgment. We are grateful for the funding from NSF (DMR-9617030) and NSF ALCOM Science and Technology Center (DMR-8920147). Thoughtful and in-depth discussions with Professor A. Keller (who passed away recently) and Dr. F. Khoury regarding this topic are gratefully acknowledged.

JA993249T